The role of climate change in regulating Arctic permafrost peatland hydrological and vegetation change over the last millennium

[1]*Hui Zhang, [1]Sanna R. Piilo, [2]Matthew J. Amesbury, [2]Dan J. Charman, [2]Angela V. Gallego-Sala, [1]Minna M. Väliranta

[1] ECRU, Department of Environmental Sciences, University of Helsinki, P.O. Box 65, 00014, Finland

[2] Geography, College of Life and Environmental Sciences, University of Exeter, UK

* Corresponding author: Email: hui.palaeo@gmail.com

Abstract

Climate warming has inevitable impacts on the vegetation and hydrological dynamics of high-latitude permafrost peatlands. These impacts in turn determine the role of these peatlands in the global biogeochemical cycle. Here, we used six active layer peat cores from four permafrost peatlands in Northeast European Russia and Finnish Lapland to investigate permafrost peatland dynamics over the last millennium. Testate amoeba and plant macrofossils were used as proxies for hydrological and vegetation changes. Our results show that during the Medieval Climate Anomaly (MCA), Russian sites experienced short-term permafrost thawing and this induced alternating dry-wet habitat changes eventually followed by desiccation. During the Little Ice Age (LIA) both sites generally supported dry-hummock habitats, at least partly driven by permafrost aggradation. However, proxy data suggest that occasionally, MCA habitat conditions were drier than during the LIA, implying that evapotranspiration may create important additional eco-hydrological feedback mechanisms under warm conditions. All sites showed a tendency towards dry conditions as inferred from both proxies starting either from *ca*. 100 years ago or in the past few decades after slight permafrost thawing, suggesting that recent warming has stimulated surface desiccation rather than deeper permafrost thawing. This study shows links between two important controls over hydrology and vegetation changes in high-latitude peatlands: direct temperature-induced surface layer response and deeper permafrost layer-related dynamics. These data provide important backgrounds for predictions of Arctic permafrost peatlands and related feedback mechanisms. Our results highlight the importance of increased evapotranspiration and thus provide an additional perspective to understanding of peatland-climate feedback mechanisms.

Keywords

Testate amoeba, plant macrofossil, hydrology, vegetation, permafrost peatlands, last millennium, MCA,

34 LIA, recent warming
35
36 **Introduction**
37 High-latitude peatlands play a critical role in the global biogeochemical cycle, through which they also
38 contribute to climate dynamics (Frolking and Roulet, 2007). Temperature and moisture balance are key
39 factors modulating peat accumulation (Carroll and Crill, 1997; Davidson and Janssens, 2006; Ovenden,
40 1990). Global warming, especially amplified warming in high-latitude regions (IPCC, 2013), is
41 expected to directly stimulate photosynthesis and net primary productivity (NPP) in high-latitude
42 ecosystems because of increased growing season length (Charman et al., 2013). Thus, peat
43 accumulation could accelerate too (Loisel and Yu, 2013). However, higher temperatures also increase
44 peat decomposition rates through accelerated microbial activity (Dorrepaal et al., 2009; Ise et al., 2008),
45 yet there is evidence from the past that during warm periods the increase in NPP exceeded the potential
46 increase in decomposition (Charman et al., 2013). Climate scenario RCP8.5 for Arctic regions predicts
47 that precipitation will increase more than 30% at the end of the twenty-first century (Collins et al.,
48 2013), which could be beneficial for peat accumulation. However, increases in precipitation may be
49 offset by increases in evapotranspiration under higher temperatures (Yu et al., 2009). Also, seasonal
50 droughts may reduce NPP and increase decomposition (Yu et al., 2009). Moreover, habitat-specific
51 plant functional types (PFTs) that characterise different peatlands (fens and bogs) have different NPP
52 dynamics and the distribution of these communities can exert a control on peat accumulation patterns
53 (Tuittila et al., 2012). While climate may directly affect plant productivity and decomposition, it may
54 also have larger-scale impacts on the geographical distribution of peatland types (Väliranta et al.,
55 2015).
56 Arctic permafrost peatlands are sensitive to climatic changes (Gałka et al., 2017a; Lamarre et al., 2012;
57 Swindles et al., 2015a; Teltewskoi et al., 2016; Tremblay et al., 2014) and at the same time, Arctic
58 permafrost peatlands affect local microclimate, hydrology, vegetation, peat and carbon accumulation
59 and these non-climatic factors again influence the degradation and aggradation of permafrost (Zuidhoff
60 and Kolstrup, 2000). Due to pronounced microtopography and persisting ice, eco-hydrological
61 processes and therefore peat accumulation patterns in permafrost peatlands are complex (Oksanen,
62 2006; Oksanen et al., 2001), making the evaluation of climate change impacts on these environments
63 challenging.
64 Northern Hemisphere mean annual temperature for the last 30- and 50-year periods is likely higher
65 than any other 30- and 50-year periods during the past 800 years (Masson-Delmotte et al., 2013).
66 Permafrost ground temperature monitoring studies have documented a rising trend over the last 20-30

years and observations suggest permafrost thaw in the southern margins of the permafrost area (Brown and Romanovsky, 2008; Johansson et al., 2011; Sannel et al., 2016). Even though these observations are not ubiquitous (Brown and Romanovsky, 2008), a widespread permafrost thaw can be expected as a consequence of global warming (Chadburn et al., 2017). It may be speculated that Arctic permafrost peatlands are on the edge of their climatological niche and have low potential to remain stable under future climate changes (Bosio et al., 2012). One presumption is that when permafrost thaws or if the active layer deepens considerably, permafrost areas become large CO_2 sources due to accelerated decomposition rates (Abbot et al., 2016; Koven et al., 2011; Schadel et al., 2016). It is suggested that these dynamics may be one of the most significant potential feedbacks from terrestrial ecosystems to the atmosphere in the future (Schuur et al., 2008). However, because of the scarcity of information and data, disentangling the links between permafrost peatland vegetation, hydrology and climate, the future balance of NPP and decomposition processes in permafrost peatlands has remained uncertain. These coupled dynamics can be investigated by comparing palaeoecological data to documented climate epochs such as the Medieval Climate Anomaly (MCA) from *ca*. AD 950-1200, the Little Ice Age (LIA) from *ca*. AD 1400-1850, and recent warming since the late 19th century (e.g., Cook et al., 2004; Esper et al., 2002; Hanhijärvi et al., 2013; Wilson et al., 2016).

In this study we investigated past hydrological changes and associated variations in vegetation composition during the last millennium in four permafrost peatlands. We used two different proxies; testate amoebae (Amesbury et al., 2016; Charman et al., 2007; Swindles et al., 2015b) and plant macrofossils (Väliranta et al., 2007; 2012) to reconstruct past moisture conditions and vegetation history, which enabled cross validation of results and therefore more dependable data interpretation (Loisel and Garneau, 2010; Väliranta et al., 2012). Using ^{14}C and ^{210}Pb dating, we linked detected changes to known climate periods. Replicate records from the same peatland and/or close-by regions allowed us to evaluate whether detected changes were climate-driven and regional or forced by autogenic factors (Mathijssen et al., 2016; 2017; Swindles et al., 2012). Our hypotheses were 1) that permafrost thawing triggered by warm climate conditions (e.g., MCA and recent warming), is reflected in proxy records as a change towards wetter plant communities and more hydrophilic testate amoeba assemblages, and that 2) permafrost aggradation under colder climate conditions such as LIA results in dry conditions through raising of the peat surface. Furthermore, we evaluate whether and how the peatland response to MCA warming differs from the on-going recent warming.

Study sites

Our four study sites are located in two regions: two sites (Indico and Seida) are located in the

discontinuous permafrost zone of Russia whereas the other two (Kevo and Kilpisjärvi) are in the sporadic permafrost zone of the Finnish Lapland (Fig. 1 and Table 1).

Indico and Seida are located in the Arctic Northeast European Russian tundra. The peat plateaus in these two peatlands are elevated a few metres from the surrounding mineral soil and the vegetation is dominated by shrub-lichen-moss communities, such as *Betula nana*, *Rhododendron tomentosum*, *Empetrum nigrum*, *Sphagnum fuscum*, *Polytrichum strictum*, *S. lindbergii* and sedges *Eriophorum* spp. Compared to Seida, Indico presents extensive areas covered by lichens and mosses with a lower shrub layer. Large bare peat surfaces occur on both sites (Repo et al. 2009).

At the two sites in Finnish Lapland, Kevo and Kilpisjärvi, the peatlands are characterised by separate permafrost mounds a few metres high and surrounding wet flarks. The mound vegetation is dominated by dwarf shrubs, such as *Betula nana*, *Empetrum nigrum*, *Rubus chamaemorus* and bryophytes *Polytrichum strictum* and *Dicranum* spp. Different *Sphagnum* species such as *S. fuscum*, *S. balticum*, *S. majus* and *S. riparium* occur along a hydrological gradient from dry hummock to wet hollow and *Eriophorum* spp. are also present.

Materials and methods

Sampling

In total, six active layer peat cores (Table 1) were collected from dry habitats either from a raised peat plateau (Russia) or from a permafrost mount (Finland) using a Russian peat corer with a diameter of 5 cm. The coring locations were dominated by dwarf shrubs, such as *Ledum palustre*, *Empetrum nigrum*, *Betula nana*, *Vaccinium uliginosum* and *Rubus chamaemorus*; or dominated by *S. fuscum*. One of the surfaces was bare with only some lichens present. Some cracking features were detected on bare/lichen-covered surface and on the edges of permafrost mounts. These can be considered as natural permafrost peatland development and life-cycle features (Seppälä, 2006). Measured active layer thickness for the studied peatlands were between 20 and 50 cm. In Indico, three replicate peat cores (Ind1-3) were collected along a transect from the centre to the margins of the site to assess potential differences in sensitivity across the peatland surface. A single core was collected from each of the other sites. Individual cores were wrapped in plastic and transported to the laboratory in sealed PVC tubes and stored in a freezer. The cores were later defrosted and sub-sampled in 1-cm or 2-cm thick slices for further analyses. In some cases, analysis of both proxies from the same sample was not possible due to a lack of material. When this occurred, analysis was carried out using stratigraphically adjacent samples. In core ‘Sei’ from Seida the limited amount of material meant that only testate amoeba analysis was possible.

133

134 *Chronology*

135 Eighteen bulk peat samples were sent to the Finnish Museum of Natural History (LUOMUS, Helsinki,
136 Finland) and the Poznan Radiocarbon Laboratory (Poznan, Poland) for accelerator mass spectrometry
137 (AMS) ^{14}C dating (Table 1). Bulk peat samples were used because of high decomposition of some peat
138 sections, which made picking out known macrofossils very difficult or impossible. Additionally, a
139 recent study suggested that there is no significant difference between ages derived from bulk material
140 and plant macrofossils in these settings (Holmquist et al., 2016). The chronology of the top parts of
141 three peat cores were determined using ^{210}Pb dating (Table 1). The samples were processed at the
142 University of Exeter, UK. A dry *ca.* 0.2-0.5 g subsample from each 1-cm interval was analyzed for
143 ^{210}Pb activity after spiking with a ^{209}Po yield tracer. The procedure followed a modified version of Ali
144 et al. (2008).
145 An age-depth model for each core was developed using CLAM 2.2 (Blaauw, 2010) in R version 3.2.4
146 (R Core Team, 2014), with ^{14}C ages internally calibrated using the INTCAL 13 calibration curve
147 (Reimer et al., 2013). ^{210}Pb ages were obtained through the Constant Rate of Supply model (CRS)
148 (Appleby and Oldfield, 1978), which was chosen over the Constant Initial Composition model because
149 there was a subsurface maximum in ^{210}Pb activity in these three cores, suggesting that the peat
150 accumulation rate has not been constant over time. Both ^{14}C and ^{210}Pb dates were included in the final
151 age-depth models (Fig. 2). A smooth spline method was selected to develop the age-depth models with
152 the exception of core Kev BS, which yielded age reversals when the default smoothing parameter 0.3
153 of CLAM model was employed and relatively large deviations of the calibrated ^{14}C dates to the
154 age-depth model curve when changing this parameter, so a linear interpolation method was used
155 instead for that core. Calibrated radiocarbon ages were rounded to the nearest 5 years. Negative ages
156 indicate post-bomb ages (i.e. -50 cal. BP = AD 2000). In this study we focused solely on the time
157 period of the last millennium.
158

159 *Testate amoeba and plant macrofossil analysis*

160 Testate amoeba sample preparation procedure followed a modified version of Booth et al. (2010).
161 Samples were boiled in distilled water for 15 minutes. Samples were sieved using a 180-μm mesh
162 instead of the standard 300-μm mesh as some materials contained a large quality of decomposed plant
163 detritus. All samples were back-sieved using a 15-μm sieve. Materials retained on the 15 μm sieve
164 were centrifuged at 3000 rpm for 5 minutes. 50-100 individual testate amoeba shells for each sample
165 were counted and identified to species level or ‘type’ under a light microscope with 200-400×

magnification. Taxonomy followed Charman et al. (2000), but occasionally online sources were used to aid identification (http://www.arcella.nl/; user.xmission.com/~psneeley/Personal/FwrPLA.htm). Occasionally the lower parts of the peat sections were highly decomposed and decomposed plant material hindered testate amoeba identification. These samples were treated with 5% KOH to disaggregate and remove fine organics before sieving (Barnett et al., 2013; Charman et al., 2010). However, because the test count did not reach 50 specimens in these deeper samples (see also Gałka et al., 2018), they were not included in the water-table depth (WTD) reconstructions.

For plant macrofossil analysis, volumetric samples (2-5 cm^3) were gently rinsed under running water using a 140- μm sieve. No chemical treatment was necessary. Remains retained on the sieve were identified and proportions of different plant types were estimated using a stereomicroscope. Further identification to species level was carried out using a high-power light microscope following Väliranta et al. (2007). In addition to identifiable plant remains, the proportion of unidentified organic matter (UOM) was also estimated.

WTD reconstruction

Testate amoeba WTD reconstructions were performed using the Rioja package (Juggins, 2015) in R version 3.2.4 (R Core Team, 2014). The modern training set contained 59 testate amoeba taxa from 145 samples collected from the same study sites (Zhang et al., 2017). A tolerance-downweighted weighted averaging with inverse deshrinking based model was applied and z scores of the reconstructed WTD values were then calculated over the total length of all the cores to illustrate hydrological changes ($z>0$ indicates drier than average conditions and $z<0$ indicates wetter than average conditions; $\triangle z=1$ represents 8.14 cm WTD range in our dataset), as the reconstructions may poorly represent actual magnitude of water table changes (Swindles et al., 2015c). Model testing and validation are discussed in Zhang et al. (2017).

Results

Chronology and vertical peat growth

Age-depth models show that peat accumulation rates have not been consistent between the study sites over the last few millennia (Fig. 2, Table 1). The thickness of active layers in four sites ranged from 31 cm to 45 cm and basal ages of active layers ranged from 1485 to 7230 cal. BP. In most cases, 25-30 cm peat thickness covered the last millennium, except in Seida where only 7 cm of peat has accumulated during the last millennium. Mean peat accumulation rates over the last millennium ranged from 0.10 to 0.81 mm/year. Vertical growth has been slower at Seida and Kilpisjärvi when compared to Indico and

Kevo.

Testate amoeba assemblages and reconstructed WTD

In total, 35 testate amoeba taxa were found in the four study sites. The most dominant taxa for all sites were *Difflugia pristis*, *Pseudodifflugia fulva* type, *P. fascicularis* type and *Trigonopyxis minuta* type (Fig. 3). In Indico *Archerella flavum*, *Cyclopyxis arcelloides* type (shell diameter around 50 µm, with an aperture >1/2 of shell diameter was applied to separate this taxon from *D. globulosa* type), *D. pulex*, *Hyalosphenia minuta* and *Nebela militars* type were also occasionally abundant, while in Seida *Assulina muscorum*, *C. arcelloides* type and *Trinema/Corythion* type were present abundantly. In Kevo *Trinema/Corythion* type was dominant in the topmost samples while in Kilpisjärvi the samples were dominated by *Arcella catinus*.

Three cores were analysed from Indico (Ind1-3), Russia. The testate amoeba assemblages of core Ind1 (Fig. 3a) were first dominated by *P. fulva* type and *D. pristis* at 985 cal. BP. After that until *ca.* 445 cal. BP *P. fulva* type was the most abundant. Between *ca.* 445 and -30 cal. BP, *P. fulva* type, *P. fascicularis* type and *C. arcelloides* type were dominant. *A. flavum* and *A. seminulum* were frequently encountered in samples before -58 cal. BP, after which the proportion of *H. minuta* increased. WTD reconstructions showed that wet conditions occurred at 985 cal. BP, after which relatively dry conditions persisted, with only slight fluctuations before *ca.* 10 cal. BP. At *ca.* 10 cal. BP, a change from dry to wet conditions was detected. After a *ca.* 50-year wet phase, a gradual transition from wet to dry occurred.

The bottom part of core Ind2 (Fig. 3b) was a mixture of peat and sand and testate amoeba were absent or scarce, so testate amoeba data were available only from *ca.* 430 cal. BP onwards. The assemblages were dominated by *C. arcelloides* type and *P. fulva* type between *ca.* 430 and 10 cal. BP but towards the core surface *N. militars* type became the dominant taxon. WTD reconstructions showed a dry-wet shift at *ca.* 175 cal. BP and a wet-dry shift at *ca.* 0 cal. BP. During the period 175-0 cal. BP, conditions were generally wet, but fluctuating. Since *ca.* 0 cal. BP an obvious drying trend prevailed.

In core Ind3 (Fig. 3c), *D. pulex* and *P. fulva* type dominated the assemblages between *ca.* 1020 and 950 cal. BP. Then *T. minuta* type became abundant until *ca.* 490 cal. BP after which *D. pristis* and *A. flavum* were the most abundant taxa until *ca*. 215 cal. BP. After that, *D. pristis, N. militars* type and *T. minuta* type were the most common taxa. The WTD reconstruction showed very dry conditions prevailed until *ca.* 400 cal. BP, when an obvious dry to wet shift occurred. However, the dominance of the medium wet indicator *D. pristis* (Zhang et al., 2017) suggests only relatively wet conditions. Starting from this shift, a slight wet to dry trend persisted until present-day.

At Seida (Fig. 3d), testate amoeba assemblages around 1060 cal. BP were dominated by *P. fulva* type,

while between *ca.* 1060 and 350 cal. BP *D. pristis* and *A. muscorum* were the most abundant taxa. Relatively wet conditions were inferred between *ca.* 650 and 350 cal. BP and after 350 cal. BP, *A. muscorum, C. arcelloides* type and *Trinema/Corythion* type were the dominant taxa. WTD reconstructions indicated that this site was persistently dry.

At Kevo (Fig. 3e), the assemblage was dominated by *P. fulva* type for the period *ca.* 1140-100 cal. BP, then *T. minuta* type and *T. arcula* type became abundant between *ca.* 100 to -20 cal. BP. Towards the surface, *T. minuta* type together with *Trinema/Corythion* type were the most abundant taxa. WTD reconstructions showed that dry conditions existed through the core with a relatively wet event recorded at *ca.* 550 cal. BP. A drying trend prevailed from *ca.* 50 cal. BP until present.

At Kilpisjärvi (Fig. 3f), the assemblages generally resembled those of Kevo but the timing of comparable assemblage change differed. *D. pristis*, *P. fulva* type and *P. fascicularis* type were abundant between *ca.* 1080 and 450 cal. BP. Large proportions of *D. pristis* and *T. minuta* type were recorded between *ca.* 450 and 0 cal. BP, with *A. catinus* and *T. minuta* types dominant towards recent times. Interestingly, some samples (18-23 cm) contained large quantities of diatoms including taxa such as *Pinnularia major*, *Cymbopleura subcuspidata*, *Eunotia praerupta*, *Eunotia serra* and *Brachysira vitrea*. The amount of diatoms was so overwhelming that testate amoeba could not be reliably counted or identified, so these samples were omitted from the WTD reconstruction. WTD reconstructions suggested a relatively wet phase *ca.* 650-450 cal. BP after which, dry but slightly fluctuating conditions persisted until the present.

Vegetation, presence of permafrost and microtopographical evolutions

Plant assemblages varied between the cores (Fig. 3). Plant composition data were used to classify the contemporary habitat conditions and to infer the presence/absence of permafrost (e.g., Oksanen, 2006; Pelletier et al., 2017). In general, we interpret that communities dominated by sedges and brown mosses indicate permafrost-free/thaw habitats while highly decomposed peat with ericaceous/woody remains sometimes accompanied by lichens and fungi sclerotia indicate peat accumulated on top of permafrost following the up-heave of the peatland surface. Though in general Sphagna assemblages are used to shed light on moisture conditions they can also help to identify the presence or absence of permafrost. Temporal permafrost melt may create suitable conditions for wet Sphagna but these species may also represent permafrost-free hollow conditions. Dry Sphagna may grow on top of permafrost hummocks, but equally on permafrost-free hummocks. In addition, though sedges are considered non-permafrost species, some species such as *Eriophorum* spp. can grow on peat plateaus, thus more than a single indicator is usually needed to identify potential presence of permafrost (e.g., Oksanen,

2005, 2006; Oksanen et al., 2003; Pelletier et al., 2017).

At Indico, between 1300 and 985 cal. BP, hummock shrub vegetation dominated in Core Ind1 (Fig. 3a), probably indicating presence of permafrost. At around 985 cal. BP abundant sedge remains indicate wet conditions, which in turn suggest permafrost free conditions, i.e. permafrost thaw. After this, until *ca.* 10 cal. BP, a mixed sedge-shrub phase, accompanied by fungi sclerotia, prevailed and peat was highly decomposed. These together suggest re-establishment of permafrost. From *ca*. 10 to -40 cal. BP, a wet hollow phase, dominated by *S. majus* and *Warnstorfia* spp., occurred and this might indicate temporary thaw of permafrost. This wet phase was followed by hummock conditions with *S. fuscum*, suggesting permafrost re-aggradation.

Ind2 (Fig. 3b) had a similar succession history, yet the timing differed. A highly decomposed Ericales stage with presence of fungi sclerotia between 1725 and 175 cal. BP was followed by *Eriophorum vaginatum* dominated phase at *ca*. 175 cal. BP. After that, a wetter lawn stage dominated by *S. capillifolium* and *S. balticum* prevailed until *ca*. 30 cal. BP. This pattern suggests alternating permafrost aggradation and melting. Similarly, the near-surface layers were dominated by *S. fuscum*, indicating permafrost re-establishment.

Ind3 (Fig. 3c) vegetation succession differed from the other two Indico records. A highly decomposed Ericales stage occupied peat layers dated to *ca.* 1020-880 cal. BP suggesting hummock conditions with permafrost underneath. Interestingly, after 880 cal. BP there was a community shift where Ericales were replaced by other hummock communities, now dominated by *S. fuscum.* This phase lasted until *ca.* 235 cal. BP. Due to a limited amount of material, we have no continuous plant macrofossil data for the time-window from 215 cal. BP to present day (-52 cal. BP). Currently dwarf shrubs Ericales grow at the coring location.

At Kevo (Fig. 3e), a mixed sedge-shrub vegetation characterised the entire peat core, suggesting that no major hydrological changes have taken place in the recent past. However, after *ca.* 380 cal. BP the plant mixture was accompanied by lichens probably suggesting permafrost conditions.

At Kilpisjärvi (Fig. 3f), before *ca.* 790 cal. BP sedges were the most dominant taxa but occasionally accompanied by other taxa such as Bryophyta spp. This community suggests a typical permafrost-free fen. The short period between *ca*. 790 and 550 cal. BP was dominated by hummock species *S. fuscum*. The following stage, which started at *ca.* 550 cal. BP and lasted until present was dominated by Ericales spp. and indicated relatively stable hummocky conditions on top of permafrost.

Discussion

MCA-induced permafrost thaw and desiccation

In NE European Russia, extensive regional-scale permafrost aggradation occurred from *ca.* 2200 cal. BP onwards (Hugelius et al., 2012; Routh et al., 2014). Therefore, we should be able to detect potential MCA-induced permafrost dynamics and hydrological changes in our Russian cores, even though regional MCA signal may be relatively weak (Briffa et al., 2013; Luoto et al., 2017). Our records suggest that at first, the MCA warming resulted in permafrost melting and consequent establishment of fen-type communities or *Sphagnum*, which corresponds to previous European Russian studies (Routh et al., 2014). At Indico (Ind1) there was a vegetation change from shrub vegetation to sedges, corresponding with the wet conditions reconstructed from testate amoebae (Figs. 3a and 4). Core Ind3 shows a transition from shrub community to *S. fuscum* at *ca.* 900 cal. BP. (Figs. 3c and 4). This kind of *Sphagnum* establishment has been proposed to be a result of warming and altered peatland hydrology and chemistry (Loisel and Yu, 2013). However, here the relatively dry conditions implied by *S. fuscum* contrasts our first hypothesis, possibly due to only partial permafrost thaw. Wet communities were replaced by shrub communities and supported by testate amoeba reconstructed dry conditions which prevailed for the latter part of the MCA (Figs. 3a and 3c). This phenomenon may either result from melt water drainage (Wilson et al., 2017), or be caused by increased evaporation (Swindles et al., 2015a).

In Fennoscandia, our results suggest that Kevo and Kilpisjärvi peatlands stayed permafrost free until *ca.* 600 cal. BP (see also Oksanen 2006). It has been suggested that during the MCA, the temperature was actually *c*. 0.5 °C lower than at present (Luoto and Nevalainen, 2017). Our data suggest that during the MCA relatively dry habitat prevailed at Kevo, while at Kilpisjärvi a wet fen prevailed (Figs. 3e and 3f). Interestingly, the samples from Kilpisjärvi dated *ca.* 970-630 cal. BP contained large amounts of diatoms and chronologically this clearly wet phase corresponds to a diatom bloom event reported from a northern Swedish peatland (Kokfelt et al., 2009; 2016). Kokfelt et al. (2016) suggested that this wet phase was likely due to the Samalas volcanic eruption in AD 1257 (693 cal. BP) and consequent acid deposition, which resulted in changes in vegetation. Therefore, the vegetation change at around 790 cal. BP from rich fen plant communities to *S. fuscum*-dominated habitat may have been triggered by volcanic impact rather than permafrost aggradation.. However, none of the other peat sections analyzed for this study have diatom-rich layers or conspicuous plant community or moisture shifts dated to around the time of the eruption. During this time period typically dry shrubby conditions prevailed in the other sites, which may have been less sensitive to acid deposition.

LIA-induced permafrost aggradation and drying

In NE European Russia, in line with our second hypothesis, plant data suggest relatively stable dry

hummocky habitats during the LIA, whereas testate amoeba data mainly indicate dry conditions, with occasional wet phases (Figs. 3 and 4). The discrepancies between the two proxies suggest testate amoeba are more sensitive to environmental changes than plant communities (Gałka et al., 2017b; Loisel and Garneau, 2010; Väliranta et al., 2012). These synchronous wet shifts in testate amoeba records at around 450-400 and 175 cal. BP (Fig. 4) contradict our second hypothesis of dry LIA conditions. However, the timing of wet phases corresponds to many other wet records registered, for example, in parts of northwest and central Europe (Charman et al., 2006; Gałka et al., 2014; Väliranta et al., 2007). These climate-caused wet interruptions failed to trigger vegetation changes with the exception of the Ind2 record, which showed a plant community change from shrubs to sedges dated to c. 175 cal. BP. This possibly suggests a greater sensitivity of peatland margins to environmental changes, as core Ind2 was collected from a more marginal location than Ind1 and 3.

Unlike at Indico and Seida, the beginning of LIA at Kilpisjärvi and Kevo seems to have been wet, which corresponds to the humid climate recorded in other parts of Finland (Väliranta et al. 2007 and references therein). Consistent with our second hypothesis, conditions subsequently shift and remain dry for the rest of the LIA *ca*. 550-100 cal. BP, most evident in testate amoeba records. Plant macrofossil data from Kilpisjärvi also support this shift by showing a vegetation change from *Sphagnum* domination to a dwarf shrub community, whilst at Kevo the drying reflected by testate amoeba data failed to cause clear vegetation changes (Figs. 3e and 3f). In contrast, according to previous studies from Kevo (e.g., Oksanen 2006), LIA triggered permafrost initiation led to dry elevated peat surfaces and vegetation changes, highlighting that one single peat core sometimes cannot capture a comprehensive regional story (University of Leeds Peat Club 2017). At Kilpisjärvi, a marked change to dry conditions indicated by testate amoeba records happened around 175 cal. BP but this is absent at Kevo. This dry phase contrasts the wet shifts at Indico and Seida, suggesting that the drivers of these changes were more regional in scale.

Implications of recent warming

Interestingly, our data consistently suggest a habitat change towards drier communities in recent decades, contradicting our first hypothesis that warming results in wetting. The drying is reflected as a change from wet *Sphagna* to dry *Sphagna* (Ind1 and 2), from *Sphagnum* spp. to Ericales shrubs (Ind3) or by an appearance of lichens and dry bryophyte taxa (Kev BS; Fig. 3). Additional testate amoeba data from Seida, Russia also repeat this pattern (Fig. S1). Chronologically, this habitat change corresponds to extensive permafrost degradation reported for the last *ca.* 50 years elsewhere (Sannel and Kuhry, 2011; Swindles et al., 2015a). Local instrumental temperature data from both regions show increasing

mean annual temperatures in recent decades (Bekryaev et al., 2010; Bulygina and Razuvaev, 2012; Mikkonen et al., 2015). In general the current mean annual temperature in northeast European Russian regions still remains below 0 °C. However, recently some individual years have approached 0 °C: e.g., years 2007 and 2004 when the annual temperature was 0.4 and -0.7 °C, respectively). Moreover, in Finnish Lapland the mean annual temperature has been above 0 °C more frequently (data from the nearest meteorological station measurements mentioned in Table 1) and warming is projected to continue (Collins et al., 2013). This may have two-fold consequences for permafrost peatlands: accelerated wetting due to thawing of permafrost but followed by desiccation afterwards due to draining and/or an increase in evapotranspiration. Such dynamics were recorded in Ind1 and Ind2 for the recent period, where permafrost thawing caused wet *S. majus*, *S. balticum and S. capillifolium* (Oksanen et al., 2003) establishment, which were later replaced by dry *S. fuscum*. The final permafrost degradation could lead to a formation of a northern fen-type environment (Swindles et al. 2015a), but only of the surface falls in surface height further as a result of loss of ice.

Conclusions

Our study emphasises the complex nature and variable sensitivity of permafrost peatlands even within a single site, and highlights the need for a multiproxy approach to environmental change reconstructions. Although hydrological and vegetation reconstructions of six cores showed some core-specific dynamics, when put together our data suggest that in general, LIA conditions were dry, supporting hummocky conditions on top of permafrost. Furthermore, we infer that conspicuous short wet events occurred as a result of the MCA and recent warming, which triggered permafrost thawing. However, some of the hydrological conditions during the MCA were drier than those of during the LIA and recent warming is associated with drier conditions across all sites even where thawing initially led to wetter conditions. The changes towards drier conditions during both the MCA and over the last 150 years suggest that evapotranspiration is an important factor in regulating surface peatland moisture conditions during warm periods in the subarctic.

The hydrological changes during the most recent warming led to especially pronounced drying of the peat surfaces following thawing, even where initial thaw caused temporarily wetter surfaces. We suggest that drying is more likely to occur where limited permafrost is present, because initial increased surface wetness caused by thawing and surface collapse will be relatively minor, and can revert to drier conditions driven by increased evapotranspiration. Whilst it is likely that continued future warming will result in extensive permafrost degradation and subseqent increased surface wetness and Arctic fen development at the landscape-level, our data show that permafrost peatland

ecosystems may also respond in more complex ways, including drying. Future changes in precipitation and evapotranspiration are more uncertain than temperature rise, but may be critical in determinng future hydrology and vegetation shifts in permafrost peatlands.

Acknowledgements

HZ acknowledges the support of the China Scholarship Council for her PhD study (grant no. 201404910499) at the University of Helsinki. Further funding was provided by the Academy of Finland, the University of Helsinki and the Natural Environment Research Council, UK (NERC Standard grant NE/I012915/1) Nicole Sanderson helped with ^{210}Pb analyses, Jaakko Leppänen provided cartographical help, Paul Mathijssen, Tiina Ronkainen and Pirita Oksanen assisted with fieldwork, and Jan Weckström identified the diatoms. We thank Tiina Ronkainen for her comments on the early version of the manuscript.

References

Abbott, B.W., Jones, J.B., Schuur, E.A.G., Chapin III, F.S., Bowden, W.B., Bret-Harte, M.S., Epstein, H.E., Flannigan, M.D., Harms, T.K., Hollingsworth, T.N., Mack, M.C., McGuire, A.D., Natali, S.M., Rocha, A.V., Tank, S.E., Turetsky, M.R., Vonk, J.E., Wickland, K.P., Aiken, G.R., Alexander, H.D., Amon, R.M.W., Benscoter, B.W., Bergeron, Y., Bishop, K., Blarquez, O., Bond-Lamberty, B., Breen, A.L., Buffam, I., Cai, Y.H., Carcaillet, C., Carey, S.K., Chen, J.M., Chen, H.Y.H., Christensen, T.R., Cooper, L.W., Cornelissen, J.H.C., de Groot, W.J., DeLuca, T.H., Dorrepaal, E., Fetcher, N., Finlay, J.C., Forbes, B.C., French, N.H.F., Gauthier, S., Girardin, M.P., Goetz, S.J., Goldammer, J.G., Gough, L., Grogan, P., Guo, L.D., Higuera, P.E., Hinzman, L., Hu, F.S., Hugelius, G., Jafarov, E.E., Jandt, R., Johnstone, J.F., Karlsson, J., Kasischke, E.S., Kattner, G., Kelly, R., Keuper, F., Kling, G.W., Kortelainen, P., Kouki, J., Kuhry, P., Laudon, H., Laurion, I., Macdonald, R.W., Mann, P.J., Martikainen, P.J., McClelland, J.W., Molau, U., Oberbauer, S.F., Olefeldt, D., Paré, D., Parisien, M-A., Payette, S., Peng, C.H., Pokrovsky, O.S., Rastetter, E.B., Raymond, P.A., Raynolds, M.K., Rein, G., Reynolds, J.F., Robard, M., Rogers, B.M., Schädel, C., Schaefer, K., Schmidt, I.K., Shvidenko, A., Sky, J., Spencer, R.G.M., Starr, G., Striegl, R.G., Teisserenc, R., Tranvik, L.J., Virtanen, T., Welker, J.M., Zimov, S., 2016. Biomass offsets little or none of permafrost carbon release from soil, streams, and wildfire: an expert assessment. Environ. Res. Lett. 11, doi:10.1088/1748-9326/11/3/034014.

Ali, A.A., Ghaleb, B., Garneau, M., Asnong, H., Loisel, J., 2008. Recent peat accumulation rates in minerotrophic peatlands of the Bay James region, Eastern Canada, inferred by ^{210}Pb and ^{137}Cs radiometric techniques. Appl. Radiat. Isot. 66, 1350-1358.

Akerman, H.J., 1998. Active layer monitoring, Abisko area, Sweden. In: International Permafrost Association, Data and Information Working Group, comp. Circumpolar Active-Layer Permafrost System (CAPS), version 1.0. CD-ROM available from National Snow and Ice Data Center, Boulder, Colorado: NSIDC, University of Colorado at Boulder.

Akerman, H.J., Johansson, M., 2008. Thawing Permafrost and Thicker Active Layers in Sub-arctic Sweden. Permafrost Periglacial Process. 19, 279–292.

Amesbury, M.J., Swindles, G.T., Bobrov, A., Charman, D.J., Holden, J., Lamentowicz, M., Mallon, G., Mazei, Y., Mitchell, E.A.D., Payne, R.J., Roland, T.P., Turner, T.E., Warner, B.G., 2016. Development of a new pan-European testate amoeba transfer function for reconstructing peatland palaeohydrology. Quat. Sci. Rev. 152, 132-151.

Appleby, P.G., Oldfield, F., 1978. The calculation of ^{210}Pb dates assuming a constant rate of supply of unsupported ^{210}Pb to the sediment. Catena 5, 1-8.

Barnett, R.L., Charman, D.J., Gehrels, W.R., Saher, M.H., Marshall, W.A., 2013. Testate amoebae as sea-level indicators in Northwestern Norway: developments in sample preparation and analysis. Acta Protozool. 52, 115-128.

Bekryaev, R.V., Polyakov, I., Alexeev, V.A., 2010. Role of polar amplification in long-term surface air temperature variations and modern arctic warming. J. clim. 23, 3888-3906.

Blaauw, M., 2010. Methods and code for 'classical' age-modelling of radiocarbon sequences. Quat. Geochronol. 5, 512-518.

Booth, R.K., Lamentowicz, M., Charman, D.J., 2010. Preparation and analysis of testate amoebae in peatland palaeoenvironmental studies. Mires and Peat 7, 1-7.

Bosio, J., Johansson, M., Callaghan, T.V., Johansen, B., Christensen, T.R., 2012. Future vegetation changes in thawing subarctic mires and implications for greenhouse gas exchange-a regional assessment. Clim. Change 115, 379-398.

Briffa, K.R., Melvin, T.M., Osborn, T.J., Hantemirov, R.M., Kirdyanov, A.V., Mazepa, V.S., Shiyatov, S.G., Esper, J., 2013. Reassessing the evidence for tree-growth and inferred temperature change during the Common Era in Yamalia, northwest Siberia. Quat. Sci. Rev. 72, 83-107.

Brown, J., Ferrians, O.J., Jr., Heginbottom, J.A., Melnikov, E.S., 1998. revised February 2001. Circum-arctic map of permafrost and ground ice conditions. Boulder, CO: National Snow and Ice Data Center. Digital media.

Brown, J., Romanovsky, V.E., 2008. Report from the International Permafrost Association: State of Permafrost in the First Decade of the 21st Century. Permafrost Periglacial Process. 19, 255-260.

Bulygina, O.N., Razuvaev, V.N., 2012. Daily temperature and precipitation data for 518 Russian

463 meteorological stations, Carbon Dioxide Information Analysis Center, Oak Ridge National Laboratory,
464 U.S. Department of Energy, Oak Ridge, Tennessee, doi:10.3334/CDIAC/cli.100.
465 Carroll, P., Crill, P., 1997. Carbon balance of a temperate poor fen. Glob. Biogeochem. Cycle 11,
466 349-356.
467 Chadburn, S.E., Burke, E.J., Cox, P.M., Friedlingstein, P., Hugelius, G., Westermann, S., 2017. An
468 observation-based constraint on permafrost loss as a function of global warming. Nat. Clim. Chang. 7,
469 340-344.
470 Charman, D.J., Beilman, D.W., Blaauw, M., Booth, R.K., Brewer, S., Chambers, F.M., Christen, J.A.,
471 Gallego-Sala, A., Harrison, S.P., Hughes, P.D.M., Jackson, S.T., Korhola, A., Mauquoy, D., Mitchell,
472 F.J.G., Prentice, I.C., van der Linden, M., De Vleeschouwer, F., Yu, Z.C., Alm, J., Bauer, I.E., Corish,
473 Y.M.C., Garneau, M., Hohl, V., Huang, Y., Karofeld, E., Le Roux, G., Loisel, J., Moschen, R., Nichols,
474 J.E., Nieminen, T.M., MacDonald, G.M., Phadtare, N.R., Rausch, N., Sillasoo, U., Swindles, G.T.,
475 Tuittila, E.S., Ukonmaanaho, L., Väliranta, M., van Bellen, S., van Geel, B., Vitt, D.H., Zhao, Y., 2013.
476 Climate-related changes in peatland carbon accumulation during the last millennium. Biogeosciences
477 10, 929-944.
478 Charman, D.J., Blundell, A., ACCROTELM members., 2007. A new European testate amoebae transfer
479 function for palaeohydrological reconstruction on ombrotrophic peatlands. J. Quat. Sci. 22, 209-221.
480 Charman, D.J., Blundell, A., Chiverrell, R.C., Hendon, D., Langdon, P.G., 2006. Compilation of
481 non-annually resolved Holocene proxy climate records: stacked Holocene peatland palaeo-water table
482 reconstructions from northern Britain. Quat. Sci. Rev. 25, 336-350.
483 Charman, D.J., Gehrels, W.R., Manning, C., Sharma, C., 2010. Reconstruction of recent sea-level
484 change using testate amoebae. Quat. Res. 73, 208-219.
485 Charman, D.J., Hendon, D., Woodland, W.A., 2000. The Identification of Testate Amoebae (Protozoa:
486 Rhizopoda) in Peats. Quaternary Research Association, Oxford.
487 Collins, M., Knutti, R., Arblaster, J., Dufresne, J-L., Fichefet, T., Friedlingstein, P., Gao, X., Gutowski,
488 W.J., Johns, T., Krinner, G., Shongwe, M., Tebaldi, C., Weaver, A.J., Wehner, M., 2013. Long-term
489 Climate Change: Projections, Commitments and Irreversibility, In: Stocker, T.F., Qin, D., Plattner, G-K.,
490 Tignor, M., Allen, S.K., Boschung, J., Nauels, A, Xia, Y., Bex, V., Midgley, P.M. (Eds.), Climate
491 Change 2013: The Physical Science Basis. Contribution of Working Group I to the Fifth Assessment
492 Report of the Intergovernmental Panel on Climate Change. Cambridge University Press, Cambridge,
493 United Kingdom and New York, NY, USA.
494 Cook, E.D., Esper, J., D'Arrigo, R.D., 2004. Extra-tropical Northern Hemisphere land temperature
495 variability over the past 1000 years. Quat. Sci. Rev. 23, 2063-2074.

Davidson, E.A., Janssens, I.A., 2006. Temperature sensitivity of soil carbon decomposition and feedbacks to climate change. Nature 440, 165-173.

Dorrepaal, E., Toet, S., van Logtestijn, R.S.P., Swart, E., van de Weg, M.J., Callaghan, T.V., Aerts, R., 2009. Carbon respiration from subsurface peat accelerated by climate warming in the subarctic. Nature 460, 616-619.

Esper, J., Cook, E.R., Schweingruber, F.H., 2002. Low-frequency signals in long tree-ring chronologies for reconstructing past temperature variability. Science 295, 2250-2253.

Frolking, S., Roulet, N.T., 2007. Holocene radiative forcing impact of northern peatland carbon accumulation and methane emissions. Glob. Change Biol. 13, 1079-1088.

Gałka, M., Swindles, G.T., Szal, M., Fulweber, R., Feurdean, A., 2018. Response of plant communities to climate change during the late Holocene: Palaeoecological insights from peatlands in the Alaskan Arctic. Ecol. Indic. 85, 525-536.

Gałka, M., Szal, M., Watson, E.J., Gallego-Sala, A., Amesbury, M.J., Charman, D.J., Roland, T.P., Turner, T.E., Swindles, G.T., 2017a. Vegetation Succession, Carbon Accumulation and Hydrological Change in Subarctic Peatlands, Abisko, Northern Sweden. Permafrost Periglacial Process. doi: 10.1002/ppp.1945.

Gałka, M., Tobolski, K., Górska, A., Lamentowicz, M., 2017b. Resilience of plant and testate amoeba communities after climatic and anthropogenic disturbances in a Baltic bog in Northern Poland: Implications for ecological restoration. Holocene 27, 130-141.

Gałka, M., Tobolski, K., Górska, A., Milecka, K., Fiałkiewicz-Kozieł, B., Lamentowicz, M., 2014. Disentangling the drivers for the development of a Baltic bog during the Little Ice Age in northern Poland. Quat. Int. 328–329, 323–337.

Hanhijärvi, S., Tingley, M.P., Korhola, A., 2013. Pairwise comparisons to reconstruct mean temperature in the Arctic Atlantic Region over the last 2,000 years. Clim. Dyn. 41, 2039–2060.

Holmquist, J.R., Finkelstein, S.A., Garneau, M., Massa, C., Yu, Z.C., MacDonald, G.M., 2016. A comparison of radiocarbon ages derived from bulk peat and selected plant macrofossils in basal peat cores from circum-arctic peatlands. Quat. Geochronol. 31, 53-61.

Hugelius, G., Routh, J., Kuhry, P., Crill, P., 2012. Mapping the degree of decomposition and thaw remobilization potential of soil organic matter in discontinuous permafrost terrain. J. Geophys. Res. 117, G02030, doi:10.1029/2011JG001873.

IPCC, 2013. Summary for Policymakers, In: Stocker, T.F., Qin, D., Plattner, G-K., Tignor, M., Allen, S.K., Boschung, J., Nauels, A, Xia, Y., Bex, V., Midgley, P.M. (Eds.), Climate Change 2013: The Physical Science Basis. Contribution of Working Group I to the Fifth Assessment Report of the

529 Intergovernmental Panel on Climate Change. Cambridge University Press, Cambridge, United
530 Kingdom and New York, NY, USA.
531 Johansson, M., Åkerman, J., Keuper, F., Christensen, T.R., Lantuit, H., Callaghan, T.V., 2011. Past and
532 present permafrost temperatures in the Abisko Area: redrilling of boreholes. Ambio 40, 558-565.
533 Juggins, S., 2015. Rioja: Analysis of Quaternary ScienceData, R package version (0.9-5).
534 (http://cran.r-project.org/package=rioja).
535 Kaverin, D.A., Pastukhov, A.V., Lapteva, E.M., Biasi, C., Marushchak, M., Martikainen, P., 2016.
536 Morphology and Properties of the Soils of Permafrost Peatlands in the Southeast of
537 the Bol'shezemel'skaya Tundra. Eurasian Soil Sci. 49, 498–511.
538 Kokfelt, U., Muscheler, R., Mellstrom, A., Struyf, E., Rundgren, M., Wastegard, S., Hammarlund, D.,
539 2016. Diatom blooms and associated vegetation shifts in a subarctic peatland: responses to distant
540 volcanic eruptions? J. Quat. Sci. 31, 723-730.
541 Kokfelt, U., Struyf, E., Randsalu, L., 2009. Diatoms in peat–Dominant producers in a changing
542 environment? Soil Biol. Biochem. 41, 1764-1766.
543 Koven, C.D., Ringeval, B., Friedlingstein, P., Ciais, P., Cadule, P., Khvorostyanov, D., Krinner, G.,
544 Tarnocai, C., 2011. Permafrost carbon-climate feedbacks accelerate global warming. Proc. Natl. Acad.
545 Sci. U.S.A. 108, 14769-14774.
546 Lamarre, A., Garneau, M., Asnong, H., 2012. Holocene paleohydrological reconstruction and carbon
547 accumulation of a permafrost peatland using testate amoeba and macrofossil analyses, Kuujjuarapik,
548 subarctic Quebec, Canada. Rev. Palaeobot. Palynology 186, 131-141.
549 Loisel, J., Garneau, M., 2010. Late Holocene paleoecohydrology and carbon accumulation estimates
550 from two boreal peat bogs in eastern Canada: Potential and limits of multi-proxy archives. Paleogeogr.
551 Paleoclimatol. Paleoecol. 291, 493-533.
552 Loisel, J., Yu, Z.C., 2013. Recent acceleration of carbon accumulation in a boreal peatland, south
553 central Alaska. J. Geophys. Res. Biogeosci. 118, 41-53.
554 Luoto, T.P., Kuhry, P., Holzkämper, S., Solovieva, N., Self, A.E., 2017. A 2000-year record of lake
555 ontogeny and climate variability from the north-eastern European Russian Arctic. Holocene 27,
556 339-348.
557 Luoto, T.P., Nevalainen, L., 2017. Quantifying climate changes of the Common Era for Finland. Clim.
558 Dyn. 49, 2557-2567.
559 Masson-Delmotte, V., Schulz, M., Abe-Ouchi, A., Beer, J., Ganopolski, A., González Rouco, J.F.,
560 Jansen, E., Lambeck, K., Luterbacher, J., Naish, T., Osborn, T., Otto-Bliesner, B., Quinn, T., Ramesh,
561 R., Rojas, M., Shao, X., Timmermann, A., 2013. Information from Paleoclimate Archives, In: Stocker,

562 T.F., Qin, D., Plattner, G-K., Tignor, M., Allen, S.K., Boschung, J., Nauels, A, Xia, Y., Bex, V., Midgley,
563 P.M. (Eds.), Climate Change 2013: The Physical Science Basis. Contribution of Working Group I to the
564 Fifth Assessment Report of the Intergovernmental Panel on Climate Change. Cambridge University
565 Press, Cambridge, United Kingdom and New York, NY, USA.
566 Mathijssen, P.J.H., 2016. Holocene carbon dynamics and atmospheric radiative forcing of different
567 types of peatlands in Finland. PhD thesis, Dep. Of Environ. Sci., Univ. of Helsinki, Finland. [Available
568 at http://hdl.handle.net/10138/161250.]
569 Mathijssen, P.J.H., Kähkölä, N., Tuovinen, J-P., Lohila, A., Minkkinen, K., Laurila, T., Väliranta, M.,
570 2017. Lateral expansion and carbon exchange of a boreal peatland in Finland resulting in 7000 years of
571 positive radiative forcing. J. Geophys. Res. Biogeosci., doi: 10.1002/2016JG003749.
572 Mazhitova, G.G., Malkova, G.V., Chestnykh, O., Zamolodchikov, D., 2004. Active-layer spatial and
573 temporal variability at European Russian Circumpolar-Active-Layer-Monitoring (CALM)
574 sites. Permafrost Periglacial Process.15, 123-139.
575 Mazhitova, G.G., Kaverin, D.A., 2007. Thaw depth dynamics and soil surface subsidence at
576 a Circumpolar active layer monitoring (CALM) site, the European north of Russia. Kriosfera Zemli XI,
577 20-30.
578 Mazhitova, G.G., Malkova, G.V., Chestnykh, O., Zamolodchikov, D., 2008. Recent decade thaw-depth
579 dynamics in the European Russian Arctic, Based on the Circumpolar Active Layer Monitoring (CALM)
580 Data. Proceedings of the Ninth International Conference on Permafrost, Fairbanks, Alaska, 2,
581 1155-1160.
582 Mikkonen, S., Laine, M., Mäkelä, H.M., Gregow, H., Tuomenvirta, H., Lahtinen, M., Laaksonen, A.,
583 2015. Trends in the average temperature in Finland, 1847-2013. Stoch. Environ. Res. Risk Assess. 29,
584 1521-1529.
585 Oksanen, P.O., 2005. Development of palsa mires on the northern European continent in relation to
586 Holocene climatic and environmental changes. PhD thesis, Dep. Of Biology, Univ. of Oulu, Finland.
587 [Available at http://herkules.oulu.fi/isbn9514278895/]
588 Oksanen, P.O., 2006. Holocene development of the Vaisjeaggi palsa mire, Finnish Lapland. Boreas 35,
589 81-95.
590 Oksanen, P.O., Kuhry, P., Alekseeva, R.N., 2001. Holocene development of the Rogovaya River peat
591 plateau, European Russian Arctic. Holocene 11, 25-40.
592 Oksanen, P.O., Kuhry, P., Alekseeva, R.N., 2003. Holocene development and permafrost history of the
593 Usinsk mire, northeast European Russia. Geographie physique et Quaternaire 57, 169-187.
594 Ovenden, L., 1990. Peat accumulation in Northern wetlands. Quat. Res. 33, 377-386.

595 Pelletier, N., Talbot, J., Olefeldt, D., Turetsky, M., Blodau, C., Sonnentag, O., Quinton, W.L., 2017.
596 Influence of Holocene permafrost aggradation and thaw on the paleoecology and carbon stirage of a
597 peatland complex in northwestern Canada. Holocene, doi: 10.1177/0959683617693899.
598 Pirinen, P., Simola, H., Aalto, J., Kaukoranta, J-P., Karlsson, P., Ruuhela, R., 2012. Tilastoja Suomen
599 ilmastosta 1981–2010 (Climatological statistics of Finland 1981–2010). Finnish Meteorological
600 Institute Reports, 1.
601 R Core Team, 2014. R: A language and environment for statistical computing. R Foundation for
602 Statistical Computing, Vienna, Austria. URL http://www.R-project.org/.
603 Reimer, P.J., Bard, E., Bayliss, A., Beck, J.W., Blackwell, P.G., Ramsey, C.B., Buck, C.E., Cheng, H.,
604 Edwards, R.L., Friedrich, M., Grootes, P.M., Guilderson, T.P., Haflidason, H., Hajdas, I., Hatté, C.,
605 Heaton, T.J., Hoffmann, D.L., Hogg, A.G., Hughen, K.A., Kaiser, K.F., Kromer, B., Manning, S.W.,
606 Niu, M., Reimer, R.W., Richards, D.A., Scott, E.M., Southon, J.R., Staff, R.A., Turney, C.S.M., van der
607 Plicht, J., 2013. IntCal13 and Marine13 radiocarbon age calibration curves, 0-50,000 years cal BP.
608 Radiocarbon 55, 1869-1887.
609 Repo, M.E., Susiluoto, S., Lind, S.E., Jokinen, S., Elsakov, V., Biasi, C., Virtanen, T., Martikainen, P.j.,
610 2009. Large N_2O emissions from cryoturbated peat soil in tundra. Nat. Geosci. 2, 189-192.
611 Routh, J., Hugelius, G., Kuhry, P., Filley, T., Tillman, P.K., Becher, M., Crill, P., 2014. Multi-proxy
612 study of soil organic matter dynamics in permafrost peat deposits reveal vulnerability to climate change
613 in the European Russian Arctic. Chem. Geol. 368, 104-117.
614 Sannel, A.B.K., Hugelius, G., Jansson, P., Kuhry, P., 2016. Permafrost warming in a Subarctic
615 peatland-which meteorological controls are most important? Permafrost Periglacial Process. 27.
616 177-188.
617 Sannel, A.B.K., Kuhry, P., 2011. Warming-induced destabilization of peat plateau/thermokarst lake
618 complexes. J. Geophys. Res. Biogeosci. 116, G03035, doi:10.1029/2010JG001635.
619 Schadel, C., Bader, M.K.F., Schuur, E.A.G., Biasi, C., Bracho, R., Capek, P., De Baets, S., Diakova, K.,
620 Ernakovich, J., Estop-Aragones, C., Graham, D.E., Hartley, I.P., Iversen, C.M., Kane, E.S., Knoblauch,
621 C., Lupascu, M., Martikainen, P.J., Natali, S.M., Norby, R.J., O'Donnell, J.A., Chowdhury, T.R.,
622 Santruckova, H., Shaver, G., Sloan, V.L., Treat, C.C., Turetsky, M.R., Waldrop, M.P., Wickland, K.P.,
623 2016. Potential carbon emissions dominated by carbon dioxide from thawed permafrost soils. Nat.
624 Clim. Chang. 6, 950-954.
625 Schuur, E.A.G., Bockheim, J., Canadell, J.G., Euskirchen, E., Field, C.B., Goryachkin, S.V., Hagemann,
626 S., Kuhry, P., Lafleur, P.M., Lee, H., Mazhitova, G., Nelson, F.E., Rinke, A., Romanovsky, V.E.,
627 Shiklomanov, N., Tarnocai, C., Venevsky, S., Vogel, J.G., Zimov, S.A., 2008. Vulnerability of

628 Permafrost Carbon to Climate Change: Implications for the Global Carbon Cycle. BioScience 58,
629 701-714.
630 Seppälä, M., 2006. Palsa mires in Finland. The Finnish environment 23, 155-162.
631 Swindles, G.T., Morris, P.J., Baird, A.J., Blaauw, M., Plunkett, G., 2012. Ecohydrological feedbacks
632 confound peat-based climate recontructions. Geophys. Res. Lett. 39, doi:10.1029/2012GL051500.
633 Swindles, G.T., Morris, P.J., Mullan, D., Watson, E.J., Turner, T.E., Roland, T.P., Amesbury, M.J.,
634 Kokfelt, U., Schoning, K., Pratte, S., Gallego-Sala, A., Charman, D.J., Sanderson, N., Garneau, M.,
635 Carrivick, J.L., Woulds, C., Holden, J., Parry, L., Galloway, J.M., 2015a. The long-term fate of
636 permafrost peatlands under rapid climate warming. Sci. Rep. 5, doi: 10.1038/srep17951.
637 Swindles, G.T., Amesbury, M.J., Turner, T.E., Carrivick, J.L., Woulds, C., Raby, C., Mullan, D., Roland,
638 T.P., Galloway, J.M., Parry, L., Kokfelt, U., Garneau, M., Charman, D.J., Holden, J., 2015b. Evaluating
639 the use of testate amoebae for palaeohydrological reconstruction in permafrost peatlands. Paleogeogr.
640 Paleoclimatol. Paleoecol. 424, 111-122.
641 Swindles, G.T., Holden, J., Raby, C.L., Turner, T.E., Blundell, A., Charman, D.J., Menberu, M.W.,
642 Kløve, B., 2015c. Testing peatland water-table depth transfer functions using high-resolution
643 hydrological monitoring data. Quat. Sci. Rev. 120, 107-117.
644 Teltewskoi, A., Beermann, F., Beil, I., Bobrov, A., De Klerk, P., Lorenz, S., Luder, A., Michaelis, D.,
645 Joosten, H., 2016. 4000 Years of Changing Wetness in a Permafrost Polygon Peatland (Kytalyk, NE
646 Siberia): A Comparative High-Resolution Multi-Proxy Study. Permafrost Periglacial Process. 27,
647 76-95.
648 Tremblay, S., Bhiry, N., Lavoie, M., 2014. Long-term dynamics of a palsa in the sporadic permafrost
649 zone of northwestern Quebec (Canada). Can. J. Earth Sci. 51, 500-509.
650 Tuittila, E-S., Juutinen, S., Frolking, S., Väliranta, M., Laine, A.M., Miettinen, A., Seväkivi, M-L.,
651 Quillet, A., Merilä, P., 2012. Wetland chronosequence as a model of peatland development: Vegetation
652 succession, peat and carbon accumulation. Holocene 23, 25-35.
653 University of Leeds Peat Club: Bacon, K.L., Baird, A.J., Blundell, A., Bourgault, M-A., Chapman, P.J.,
654 Dargie, G., Dooling, G.P., Gee, C., Holden, J., Kelly, T., McKendrick-Smith, K.A., Morris, P.J., Noble,
655 A., Palmer, S.M., Quillet, A., Swindles, G.T., Watson, E.J., Young, D.M., 2017. Questioning ten
656 common assumptions about peatlands. Mires Peat 19, 1-23.
657 Väliranta, M., Blundell, A., Charman, D.J., Karofeld, E., Korhola, A., Sillasoo, U., Tuittila, E-S., 2012.
658 Reconstructing peatland water tables using transfer functions for plant macrofossils and testate
659 amoebae: A methodological comparison. Quat. Int. 268, 34-43.
660 Väliranta, M., Korhola, A., Seppa, H., Tuittila, E.S., Sarmaja-Korjonen, K., Laine, J., Alm, J., 2007.

High-resolution reconstruction of wetness dynamics in a southern boreal raised bog, Finland, during the late Holocene: a quantitative approach. Holocene 17, 1093-1107.

Väliranta, M., Salonen, J.S., Heikkila, M., Amon, L., Helmens, K., Klimaschewski, A., Kuhry, P., Kultti, S., Poska, A., Shala, S., Veski, S., Birks, H.H., 2015. Plant macrofossil evidence for an early onset of the Holocene summer thermal maximum in northernmost Europe. Nat. Commun. 6, 6809.

Wilson, R., Anchukaitis, Kevin., Briffa, K.R., Büntgen, U., Cook, E., D'Arrigo, R., Davi, N., Esper, J., Frank, D., Gunnarson, B., Hegerl, G., Helama, S., Klesse, S., Krusic, P.J., Linderholm, H.W., Myglan, V., Osborn, T.J., Rydval, M., Schneider, L., Schurer, A., Wiles, G., Zhang, P., Zorita, E., 2016. Last millennium northern hemisphere summer temperatures from tree rings: Part I: The long term context. Quat. Sci. Rev. 134, 1-18.

Wilson, R.M., Fitzhugh, L., Whiting, G.J., Frolking, S., Harrison, M.D., Dimova, N., Burnett, W.C., Chanton, J.P., 2017. Greenhouse gas balance over thaw-freeze cycles in discontinuous zone permafrost. J. Geophys. Res. Biogeosci. 122, 387-404.

Yu, Z.C., Beilman, D.W., Jones, M.C., 2009. Sensitivity of Northern Peatland Carbon Dynamics to Holocene Climate Change, in: Baird, A.J., Belyea, L.R. Comas, X., Reeve, A.S., Slater, L.D. (Eds.) Carbon Cycling in Northern Peatlands. American Geophysical Union, Washington, D.C.. doi: 10.1029/2008GM000822.

Zhang, H, Amesbury, M.J., Ronkainen, T., Charman, D.J., Gallego-Sala, A.V., Väliranta, M., 2016. Testate amoeba as palaeohydrological indicators in the permafrost peatlands of Northeast European Russia and Finnish Lapland. J. Quat. Sci. doi:10.1002/jqs.2970.

Zuidhoff, F.S., Kolstrup, E., 2000. Changes in Palsa Distribution in Relation to Climate Change in Laivadalen, Northern Sweden, Especially 1960-1997. Permafrost Periglacial process. 11, 55-69.

686 Table 1 Detailed study site and core information. Mean annual temperature (MAT) and mean annual
687 precipitation (MAP) data for Indico are from Naryan-Mar meteorological station and cover the period
688 1961-1990, for Seida are from Vorkuta meteorological station covering the period 1977-2006; for Kevo
689 are from Utsjoki Kevo meteorological station and for Kilpisjärvi are from Enontekiö Kilpisjärvi
690 Kyläkeskus meteorological station (Pirinen *et al*., 2012), for the period 1981-2010.

Site	Latitude (N)	Longitude (E)	MAT (°C)	MAP (mm)	Core	ALT (cm)	Dated depth (cm)	^{14}C age (BP)
Indico, Russia	67°16′01″	49°52′59.9″	-4	501	*Ind1	35	19-20	109±22
							34-35	2066±25
					*Ind2**	45	25-26	726±24
							34-35	4105±35
							44-45	6308±33
					Ind3	44	12-14	240±30
							24-26	345±35
							42-44	1941±35
Seida, Russia	67°07′0.12″	62°57′	-5.6	501	Sei	39	8-10	560±30
							14-16	3230±35
							22-24	4245±40
							38-39	5775±38
Kevo, Finland	69°49′26.1″	27°10′20.7″	-1.3	433	Kev BS	31	0-1	105.92±0.34(pMC)
							17-18	50±30
							26-27	1540±30
							30-31	1610±30
Kilpisjärvi, Finland	68°53′4.5″	21°3′11.94″	-1.9	487	*Kil	32	17-18	600±30
							31-32	1750±30

691 * surface ages were dated by ^{210}Pb. For other sites/cores, ^{14}C date or collecting year was applied. **
692 base of core in contact with mineral soil.
693 BS represents bare peat surface, other cores are from vegetated peat surfaces. pMC represents
694 percentage modern carbon, with modern defined as AD 1950. ALT represents active layer thickness.
695
696
697

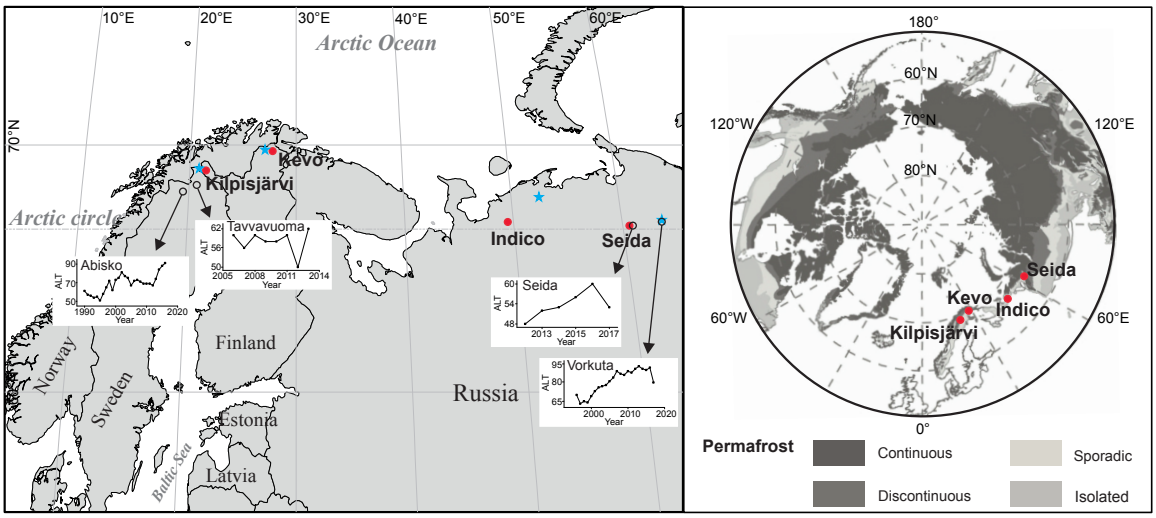

Fig. 1. Locations of the study sites (red dots). Climate data for each site are derived from the nearest meteorological station (blue stars), see details in Table 1. Active layer thickness (ALT; cm) measurements from nearby sites are shown in inset plots (Akerman 1998; Akerman and Johansson, 2008; Kaverin et al., 2016; Mazhitova et al., 2004, 2007, 2008; Sannel et al., 2016). Data for circum-Arctic permafrost zonation map are edited from Brown et al., 1998.

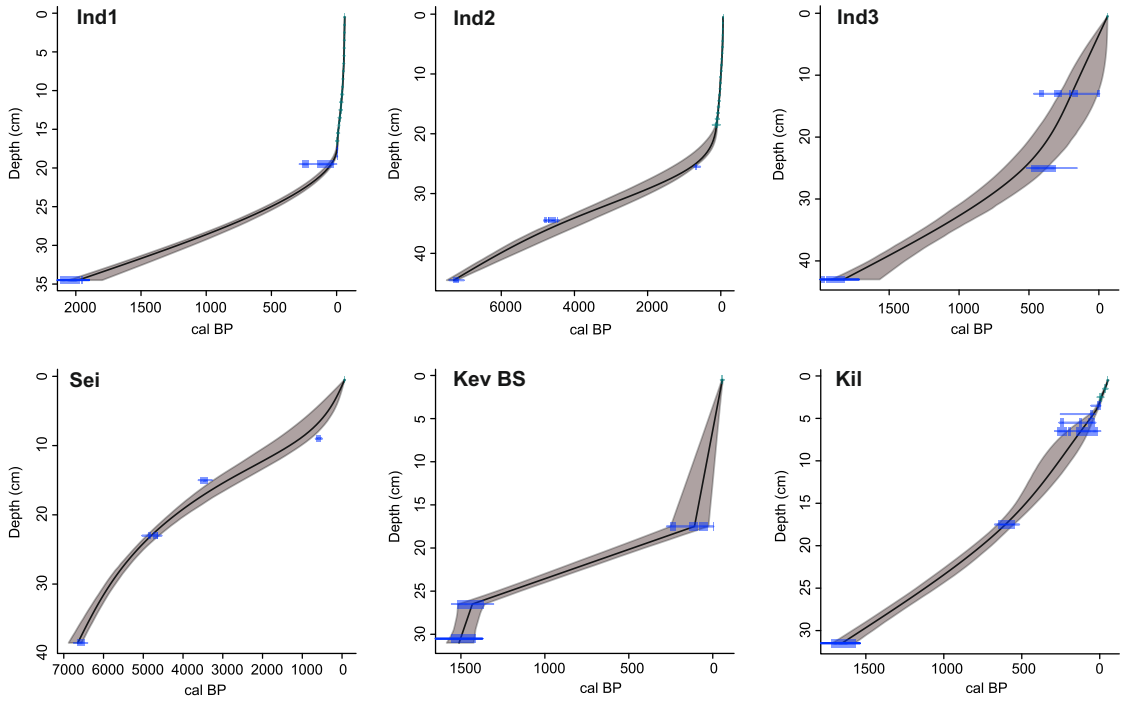

Fig. 2. Age-depth models of studied peat cores from four permafrost peatlands produced using the CLAM model.

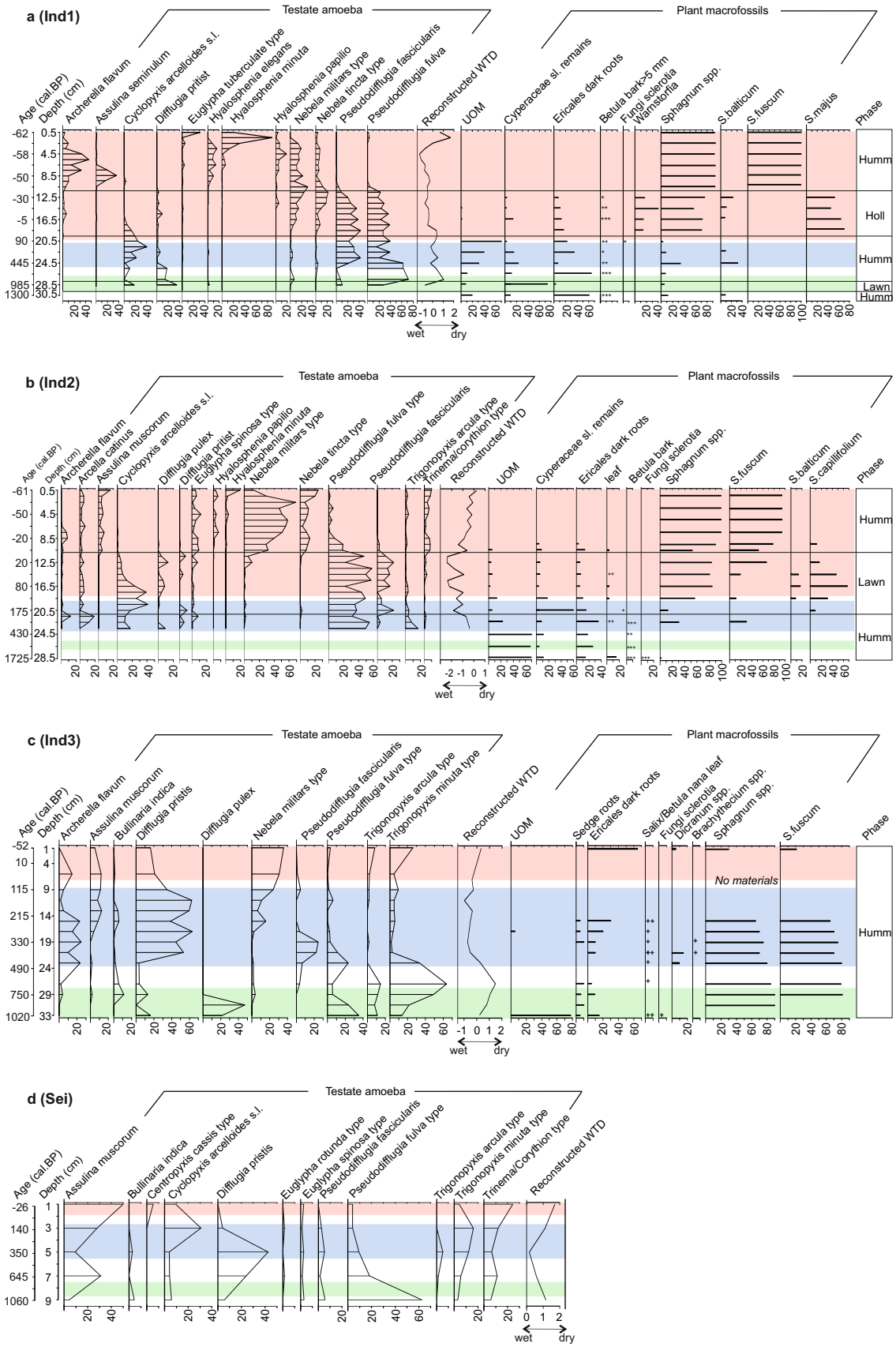
a (Ind1)
Testate amoeba
Plant macrofossils
Age (cal.BP)
Depth (cm)
Archerella flavum
Assulina seminulum
Cyclopyxis arcelloides s.l.
Difflugia pristi
Euglypha tuberculate type
Hyalosphenia elegans
Hyalosphenia minuta
Hyalosphenia papilio
Nebela militaris type
Nebela tincta type
Pseudodifflugia fascicularis
Pseudodifflugia fulva
Reconstructed WTD
UOM
Cyperaceae sl. remains
Ericales dark roots
Betula bark>5 mm
Fungi sclerotia
Warnstorfia
Sphagnum spp.
S.balticum
S.fuscum
S.majus
Phase
-62 0.5
-58 4.5
-50 8.5
-30 12.5
-5 16.5
90 20.5
445 24.5
985 28.5
1300 30.5
Humm
Holl
Humm
Lawn
Humm
wet
dry
b (Ind2)
Testate amoeba
Plant macrofossils
Age (cal.BP)
Depth (cm)
Archerella flavum
Arcella catinus
Assulina muscorum
Cyclopyxis arcelloides s.l.
Difflugia pulex
Difflugia pristi
Euglypha spinosa type
Hyalosphenia papilio
Hyalosphenia minuta
Nebela militaris type
Nebela tincta type
Pseudodifflugia fulva type
Pseudodifflugia fascicularis
Trigonopyxis arcula type
Trinema/corythion type
Reconstructed WTD
UOM
Cyperaceae sl. remains
Ericales dark roots
leaf
Betula bark
Fungi sclerotia
Sphagnum spp.
S.fuscum
S.balticum
S.capillifolium
Phase
-61 0.5
-50 4.5
-20 8.5
20 12.5
80 16.5
175 20.5
430 24.5
1725 28.5
Humm
Lawn
Humm
wet
dry
c (Ind3)
Testate amoeba
Plant macrofossils
Age (cal.BP)
Depth (cm)
Archerella flavum
Assulina muscorum
Bullinaria indica
Difflugia pristis
Difflugia pulex
Nebela militaris type
Pseudodifflugia fascicularis
Pseudodifflugia fulva type
Trigonopyxis arcula type
Trigonopyxis minuta type
Reconstructed WTD
UOM
Sedge roots
Ericales dark roots
Salix/Betula nana leaf
Fungi sclerotia
Dicranum spp.
Brachythecium spp.
Sphagnum spp.
S.fuscum
Phase
-52 1
10 4
115 9
215 14
330 19
490 24
750 29
1020 33
No materials
Humm
wet
dry
d (Sei)
Testate amoeba
Age (cal.BP)
Depth (cm)
Assulina muscorum
Bullinaria indica
Centropyxis cassis type
Cyclopyxis arcelloides s.l.
Difflugia pristis
Euglypha rotunda type
Euglypha spinosa type
Pseudodifflugia fascicularis
Pseudodifflugia fulva type
Trigonopyxis arcula type
Trigonopyxis minuta type
Trinema/Corythion type
Reconstructed WTD
-26 1
140 3
350 5
645 7
1060 9
wet
dry

713 Continued

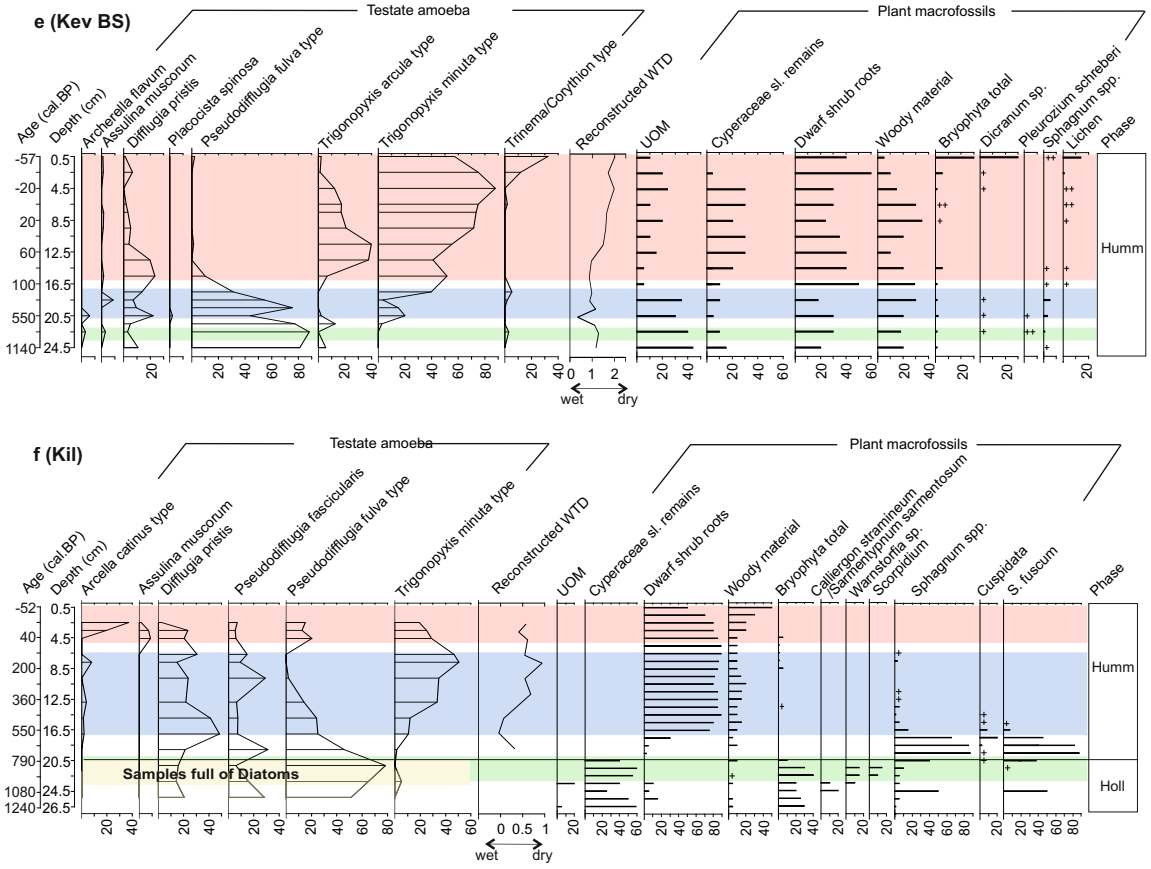

714

715 Fig. 3. Testate amoeba and plant macrofossil assemblages (selected taxa) from four permafrost peatlands. Testate amoeba-based
716 water-table depth (WTD) reconstructions are shown, data are normalized as z scores over their total length (z>0 indicates drier
717 than average conditions and z<0 indicates wetter than average conditions; △z=1 represents 8.14 cm WTD range in our dataset).
718 Microtopographical evolution of each core is divided into different phases based on plant macrofossil data (Humm: hummock;
719 Lawn; Holl: hollow). Climate phases are indicated using green (Medieval Climate Anomaly), blue (Little Ice Age) and red
720 (recent warming) boxes.

721

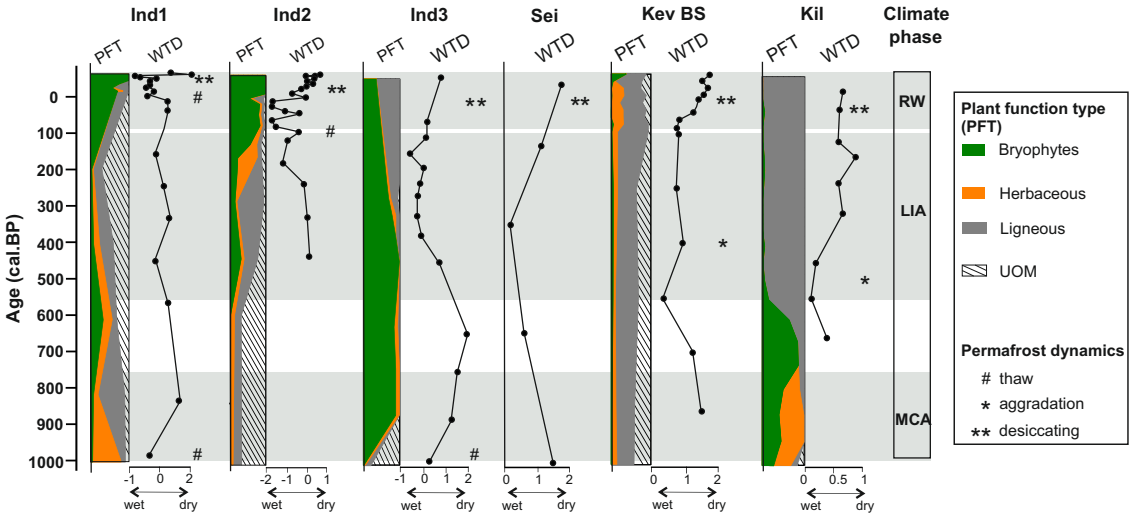

722

Fig. 4. Permafrost peatland dynamics over the last millennium. Plant function types (PFT) and reconstructed water-table depth (WTD) are presented. Main permafrost dynamics detected based on vegetation and hydrological changes are shown. MCA: Medieval Climate Anomaly; LIA: Little Ice Age; RW: recent warming.

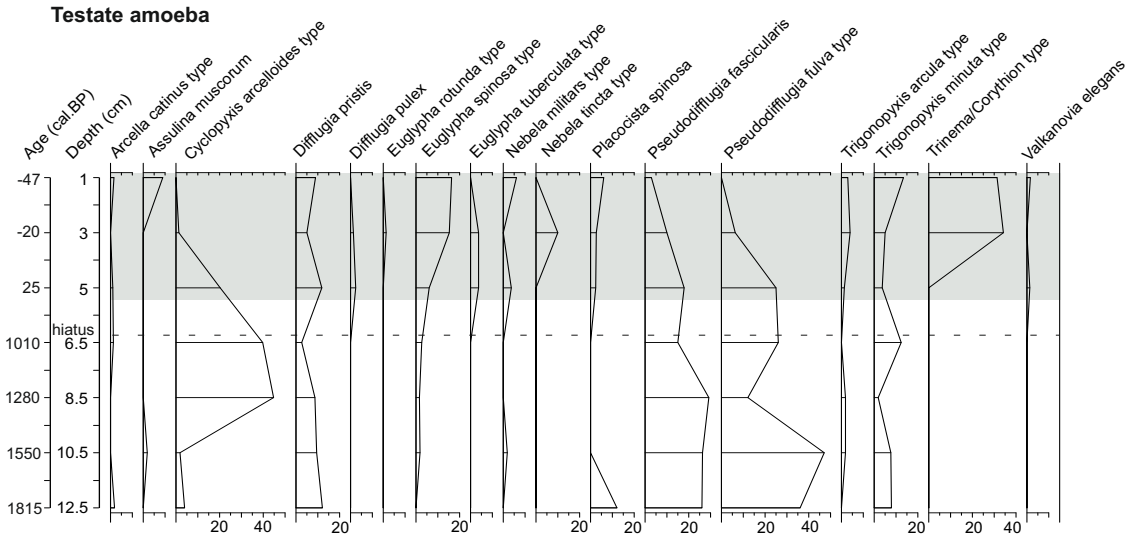

Fig. S1. Additional testate amoeba assemblages (selected taxa) from the permafrost peatland at Seida, showing shift to drier assemblages (shading section) responding to recent warming. The age-depth model of this core indicates an accumulation hiatus between *ca*. 1000-50 cal. BP, which enables only the analysis of recent decades.